Geophysical Research Letters

RESEARCH LETTER
10.1029/2020GL087621

Uncoupled El Niño Warming

Zeng-Zhen Hu[1], Michael J. McPhaden[2], Arun Kumar[1], Jin-Yi Yu[3], and Nathaniel C. Johnson[4,5]

[1]Climate Prediction Center, NCEP/NWS/NOAA, College Park, MD, USA, [2]NOAA/Pacific Marine Environment Laboratory, Seattle, WA, USA, [3]Department of Earth System Science, University of California, Irvine, CA, USA, [4]Atmospheric and Oceanic Sciences Program, Princeton University, Princeton, NJ, USA, [5]NOAA Geophysical Fluid Dynamics Laboratory, Princeton, NJ, USA

Key Points:
- Oceanic warming in the tropical Pacific is not always accompanied by corresponding atmospheric anomalies
- A weaker zonal SST anomaly gradient and a late start may partially account for the decoupling
- The impact on extratropics is different between the coupled and uncoupled warming

Supporting Information:
- Supporting Information S1

Correspondence to:
Z.-Z. Hu,
zeng-zhen.hu@noaa.gov

Citation:
Hu, Z.-Z., McPhaden, M. J., Kumar, A., Yu, J.-Y., & Johnson, N. C. (2020). Uncoupled El Niño warming. *Geophysical Research Letters*, *47*, e2020GL087621. https://doi.org/10.1029/2020GL087621

Received 21 FEB 2020
Accepted 23 MAR 2020

Abstract In light of a warming climate, the complexity of the El Niño/Southern Oscillation (ENSO) makes its prediction a challenge. In addition to various flavors of ENSO, oceanic warming in the central and eastern tropical Pacific is not always accompanied by corresponding atmospheric anomalies; that is, the atmosphere and ocean remain uncoupled. Such uncoupled warm events as happened in 1979, 2004, 2014, and 2018 are rare and represent an unusual form of ENSO diversity. A weaker zonal sea surface temperature anomaly gradient across the tropical Pacific compared to a conventional El Niño may partially account for the decoupling. Also, the uncoupled warm events typically start late in the calendar year, which raises the possible influence of seasonality in background conditions for the lack of coupling. Without coupling, the impact of the warming in the central and eastern tropical Pacific on extratropical climate is different from that of its coupled counterpart.

Plain Language Summary In a warming climate, the features of the El Niño/Southern Oscillation seem to be changing. For example, during the El Niño events in 1979, 2004, 2014, and 2018, oceanic warming in the central and eastern tropical Pacific was not accompanied by corresponding atmospheric anomalies; that is, the atmosphere and ocean remained uncoupled. These uncoupled warming events were associated with a weaker east-west contrast in sea surface temperature anomaly across the tropical Pacific compared to a conventional El Niño. Also, the uncoupled warm events typically start late in the calendar year, which raises the possible influence of seasonality in the background conditions for the lack of coupling. Without coupling, the impact of the warming in the central and eastern tropical Pacific on extratropical climate is different from that of the coupled counterpart, leading to different predictability of seasonal-interannual climate in extratropical regions, such as the United States.

1. Introduction

As the strongest climate variation in the tropics on seasonal-interannual time scales, the El Niño–Southern Oscillation (ENSO) can cause flooding, drought, heat waves, landslides, and other natural disasters that affect lives, property, economic activity, and the natural environment (National Research Council, 2010). The scientific community has made a concerted effort in studying ENSO, leading to the understanding that ENSO is the consequence of coupled interactions between the ocean and the overlying atmosphere (Bjerknes, 1969; Sarachik & Cane, 2010). The mutual reinforcement between the ocean and atmosphere is crucial for growth and amplification of anomalies in both the ocean and atmosphere. The warm phase of ENSO (El Niño) features positive sea surface temperature (SST) and subsurface ocean anomalies in the central and eastern tropical Pacific, weakened surface trade winds and Walker circulation, and an eastward shift in deep convection and rainfall. Its cold phase (La Niña) is characterized by roughly opposite oceanic and atmospheric anomalies.

In the past 50 years since the legendary work of Bjerknes (1969), substantial progress has been made in our theoretical understanding of ENSO (Sarachik & Cane, 2010), and different mechanisms to explain the ENSO cycle and its diversity have been proposed. In addition to prominent commonalities between events, ENSO also exhibits significant diversity in intensity, spatial pattern, temporal evolution, and predictability of individual events (Capotondi et al., 2015; Timmermann et al., 2018). Such diversity involves a variety of different physical processes including low-frequency deterministic time scale processes and high-frequency stochastic forcing associated with, for example, westerly wind bursts and the Madden-Julian Oscillation

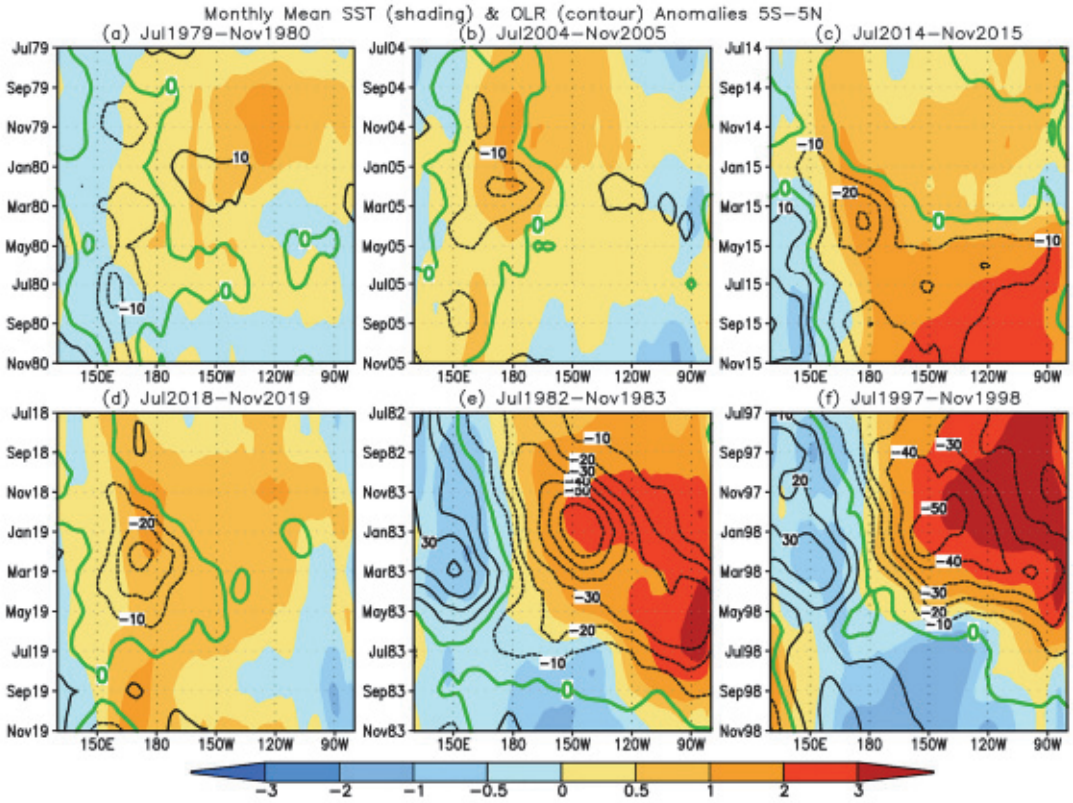

Figure 1. Evolutions of 3-month running mean sea surface temperature (SST; shading) and outgoing longwave radiation (OLR; contours) anomalies averaged between 2°S and 2°N during (a) July 1979 to November 1980, (b) July 2004 to November 2005, (c) July 2014 to November 2015, (d) July 2018 to November 2019, (e) July 1982 to November 1983, and (f) July 1997 to November 1998. The unit is °C for SST, and W/m^2 for OLR. Panels (a)–(d) correspond to uncoupled warming events, whereas (e) and (f) correspond to strong El Niño.

(e.g., Cane et al., 1990; Wang, 2018). The growth of ENSO anomalies is controlled by positive ocean-atmosphere feedbacks that involve wind stress, SST, and thermocline depth fluctuations in the tropical Pacific (Bjerknes, 1969), while the phase transition is determined by a variety of negative feedbacks (Wang, 2018). ENSO theories that have elaborated on these processes include the delayed oscillator (Battisti & Hirst, 1989; Suarez & Schopf, 1988), the recharge-discharge oscillator (Jin, 1997a, 1997b; Meinen & McPhaden, 2000; Wyrtki, 1985), the western Pacific oscillator, and the advective-reflective oscillator, respectively (Picaut et al., 1996; Wang, 2001, 2018; Wang et al., 2016).

Meanwhile, because ENSO is the major source of predictability of global climate variations on seasonal-interannual time scales (Z.-Z. Hu, Kumar, Jha, & Huang, 2020), ENSO forecasting is now operational in many climate centers around the world (Barnston et al., 2012; Zheng et al., 2016). Nevertheless, there remains an inherent challenge in predicting ENSO development and phase transitions (Z.-Z.Hu, Kumar, et al., 2019; Zheng et al., 2016) due to the small signal-to-noise ratio and the fact that random weather events (such as wind bursts) can drastically alter the course of ENSO evolution (Chen et al., 2015; McPhaden, 2015). Moreover, no steady increase in the prediction skill of ENSO has been evident in about the last 20 years (Barnston et al., 2012; McPhaden, 1999, 2015), which may be partially associated with ENSO diversity and complexity (Z.-Z. Hu, Kumar, Huang, et al., 2020; Timmermann et al., 2018) that includes eastern Pacific (EP) El Niños, central Pacific (CP) El Niños (Kao & Yu, 2009), and coastal El Niños (Z.-Z.Hu, Huang, et al., 2019). These different flavors of El Niño evolve differently and with different locations of atmospheric and oceanic anomalies that potentially affect prediction skill and impacts on extratropical climate (Z.-Z. Hu et al., 2012).

It has also been observed that the oceanic anomalous warming in the central and eastern tropical Pacific Ocean is not always accompanied by corresponding atmospheric anomalies (Figure 1). The most recent

case is 2018 (Figure 1d). The considerable warming in the central and eastern tropical Pacific during the second half of 2018 (Figure 1d) was not associated with an eastward shift of deep convection and rainfall (represented by outgoing longwave radiation, OLR) and a corresponding change of lower- and upper-level wind anomalies as typically seen in El Niño, as, for example, in 1982–1983 and 1997–1998 (Figures 1e and 1f) (Johnson et al., 2019; Li, Hu, & Huang, 2019; McPhaden, 1999, 2015; Santoso et al., 2017; Wang, 2018; Wang et al., 2016). Since ENSO is a coupled phenomenon, we term events similar to that which occurred in the latter half of 2018 as "uncoupled El Niño warming" events. In this work, we seek to understand why some El Niños do not develop readily through ocean-atmosphere feedbacks. These uncoupled warming events are rare and represent an unusual member within the spectrum of ENSO diversity in which warming in the Niño3.4 region does not readily lead to atmosphere and ocean coupling. It is not only a challenge to understand but also to characterize properly these events as well as to forecast their evolution and far-field impacts. Possible factors responsible for the lack of coupling, the effects of uncoupled warming on the extratropics, and the ability to predict these events are presented.

2. Data

Monthly mean SST is from Version 2 of the optimum interpolation SST (OIv2; Reynolds et al., 2002). Monthly mean winds at 1,000 hPa are from the National Centers for Environmental Prediction—the Department of Energy reanalysis (R2) (Kanamitsu et al., 2002). Both are on a 1° × 1° grid. Monthly mean OLR data on a 2.5° × 2.5° grid are from Liebmann and Smith (1996) to represent deep convection. Monthly mean global precipitation data on a 2.5° × 2.5° grid are from the Climate Anomaly Monitoring System (CAMS) and OLR Precipitation Index (OPI) (CAMS_OPI; Janowiak & Xie, 1999), which combines observations from rain gauges (CAMS) with satellite estimates (OPI). The heat budget for the ocean mixed layer and the depth of 20 °C isotherm (D20) is computed from the Global Ocean Data Assimilation System (Huang et al., 2010). All these data span January 1979 to December 2019, and the anomalies are computed with the reference to climatology in 1981–2010.

Prediction skill for Niño3.4 SST and zonal gradient indices are compared by using retrospective predictions (or hindcasts) for January 1982 to February 2011 and real-time predictions (or forecasts) for March 2011 to December 2018 from the National Centers for Environmental Prediction Climate Forecast System Version 2 (Saha et al., 2014). The predictions extend out to 9 months. For this analysis, we used forecasts and hindcasts from 20 initial conditions in each month to construct ensemble mean predictions.

The official forecasts of the Climate Prediction Center (CPC) for monthly mean precipitation and temperature over the United States span January 1995 to December 2019. The forecasts are expressed in three categories: above normal, near normal, and below normal, which are equally likely at any given location over thirty years. The monthly forecasts were issued on the third Thursday of the previous month. The Heidke skill score (HSS) is used to measure the accuracy of these forecasts. HSS compares how often the forecast category correctly matches the observed category, over or above the number of correct "hits" expected by chance alone (O'Lenic et al., 2008; Peng et al., 2013).

3. Ocean Warming Without Corresponding Atmospheric Anomalies

Basin-scale atmosphere-ocean coupling is normally crucial for ENSO development. However, as mentioned in section 1, ocean surface warming in the central and eastern tropical Pacific is not always linked to a basin-scale atmosphere-ocean coupling, and sometimes atmospheric disturbances alone might lead to a warm event (e.g., Clement et al., 2011; Dommenget, 2010). We define an uncoupled warming event as when SST in the central tropical Pacific is warm enough to be considered as an El Niño, but the atmospheric deep convection anomaly in the CP is absent. More specifically, we define an uncoupled warming event as an event with a monthly mean Niño3.4 index ≥0.5 °C and a Central Pacific OLR (CP_OLR) index >0.0 that persist for at least three consecutive months (Figure 2). The Niño3.4 index is defined as SST anomalies (SSTAs) averaged over 5°S to 5°N, 170–120°W (blue rectangle in Figure 3a), and the CP_OLR index is defined as OLR anomalies averaged over 5°S to 5°N, 170°E to 140°W (green rectangle in Figure 3a) following L'Heureux et al. (2015). The reason for choosing 3 months to define an uncoupled warming event is to average out short-term intraseasonal variations while capturing the processes operating in the ocean-atmosphere system that would normally lead to positive feedbacks between zonal surface winds, deep convection, and SST. This

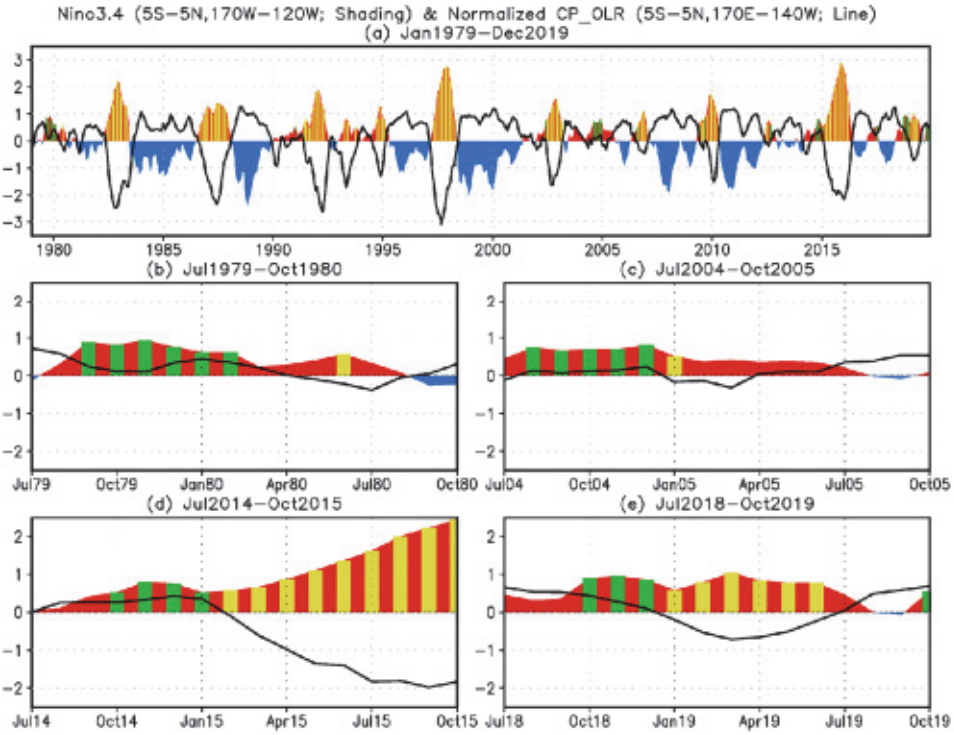

Figure 2. Time series of monthly mean Niño3.4 (red and blue shadings) and normalized CP_OLR (line) indices in (a) January 1979 to December 2019, (b) July 1979 to October 1980, (c) July 2004 to October 2005, (d) July 2014 to October 2015, and (e) July 2018 to October 2019. The green bars represent Niño3.4 ≥ 0.5 °C and CP_OLR > 0.0, and the yellow bars represent Niño3.4 ≥ 0.5 °C and CP_OLR < 0.0.

definition is similar to that used by Chiodi and Harrison (2013, 2015) to classify ENSO into events with and without accompanying OLR anomalies, namely, OLR-ENSO with an OLR anomaly averaged over the region (5°S to 5°N, 160–110°W) < −20 W/m^2, and non-OLR-ENSO with an OLR anomaly averaged over the region >−20 W/m^2. Historically, such uncoupled warming events are rare (Figure 2a), indicating that the majority of the anomalously warm events are associated with active ocean-atmosphere coupling.

According to this definition and with reference to a climatology over 1981–2010, there are four uncoupled warming events since 1979: September 1979 to February 1980, August–December 2004, October 2014 to January 2015, and October–December 2018 (see Figure 1 and the green bars in Figure 2). The results do not change if a climatology over 1979–2019 is used in computing the anomalies (not shown). The uncoupled warming events lasted ~3–6 months (Figure 2), shorter than their coupled counterparts (http://origin.cpc.ncep.noaa.gov/products/analysis_monitoring/ensostuff/ONI_v5.php). Johnson et al. (2019) noted that the uncoupled atmospheric and oceanic anomalies in the tropical Pacific Ocean associated with the weak El Niño events of 2014/2015 and 2018/2019 appeared to be rooted in the tropical SST pattern rather than internal atmospheric variability. The positive SSTAs in the four uncoupled warming events are associated with a positive thermocline depth anomaly (Figure S1 in the supporting information), suggesting that it is overall driven by oceanic dynamical processes and damped by surface heat flux (Figure S2).

In analyzing the 2014 case, McPhaden (2015) indicated that the absence of sustained feedback between zonal winds and SST was symptomatic of the atmosphere's unexpected insensitivity to warm SSTs in the central equatorial Pacific. In fact, the event of 2014 is part of the major El Niño in 2015/2016. The event of 2014 did not amplify despite a large buildup of upper ocean heat content in the equatorial Pacific because a strong easterly wind burst arrested its development. A major El Niño eventually developed in 2015 after the stalled of the 2014 event because upper heat content remained anomalously high (S. Hu & Fedorov, 2016; McPhaden, 2015). The uncoupled warming events in 1979/1980, 2004, and 2018 were followed by weak coupled warmings (Figures 1a, 1b, 1d, 2b, 2c, and 2e), and the event in 2014/2015 was followed by strong

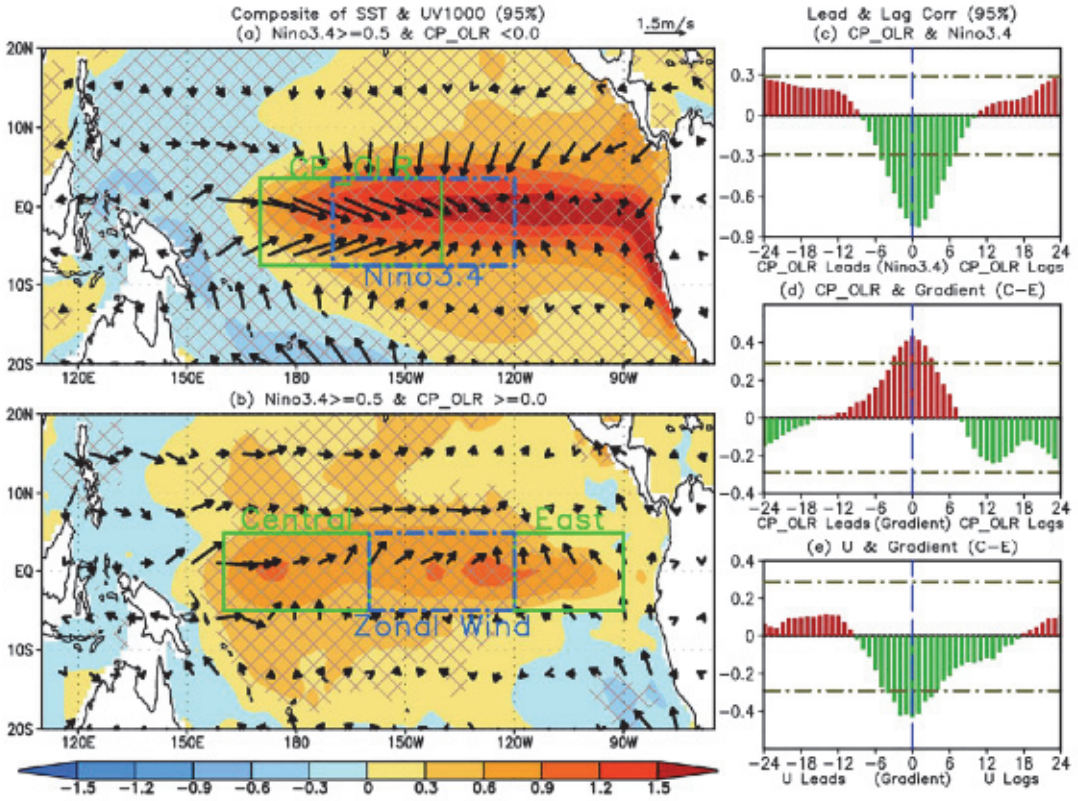

Figure 3. Composites of monthly mean anomalies of SST and wind at 1,000 hPa for (a) Niño3.4 ≥ 0.5 °C and CP_OLR < 0.0 and (b) Niño3.4 ≥ 0.5 °C and CP_OLR > 0.0 during January 1979 to December 2019. Monthly data were used in the composites, which include 111 months in (a) and 28 months in (b), respectively. The hatches indicate that the composite anomalies are significantly different at 5% level from those of the nonselected month based on a *t* test. Lead and lag correlations between (c) the CP_OLR and Niño3.4 indices, (d) the CP_OLR and SSTA zonal gradient indices, and (e) the zonal wind and SSTA zonal gradient indices. The SSTA zonal gradient index is defined as the SSTA mean difference of the central (5°S to 5°N, 160°E to 160°W) minus the eastern (5°S to 5°N, 120–90°W) tropical Pacific (the green rectangles in Figure 3b). The zonal wind index is defined as the surface zonal wind stress anomaly averaged in (5°S to 5°N, 160–120°W; the blue rectangles with dashed line in Figure 3b). The horizontal dash-dotted lines in (c)–(e) represent the 5% significance level using the *t* test with estimated independent sample size following Bretherton et al. (1999).

coupling during the El Niño in 2015/2016 (Figures 1c and 2d; Santoso et al., 2017). All four of these uncouple warming events were connected to subsequent El Niños that persisted for several seasons according to the CPC (https://origin.cpc.ncep.noaa.gov/products/analysis_monitoring/ensostuff/ONI_v5.php); it is necessary to distinguish them from coupled warm events based on their associated atmosphere and ocean variations as well as the impact on extratropical climate.

From Figure 2a, we note that compared with the uncoupled El Niño warming events, we can find no evidence for corresponding "uncoupled La Niña cooling" events. ENSO-associated atmosphere-ocean coupling requires interactions between SST, convection (as measured by precipitation or OLR) and surface wind. Convection can only occur above a certain SST threshold (Johnson & Xie, 2010); however, this SST threshold may be a necessary but not sufficient condition. Warm SSTA without favorable atmosphere conditions (such as surface wind convergence and unstable temperature stratification) would not lead to deep convection and then atmosphere-ocean coupling. For La Niña, there is no such sufficient condition for cold SSTAs. Hence, during La Niña, cold SSTA is always accompanied by suppressed deep convection and increased OLR.

A common feature of the four uncoupled warming events is that enhanced convection persisted in the western Pacific, instead of migrating eastward as expected during an El Niño (Figure 1). Physically, anomalous deep convection over the central tropical Pacific is an indicator of atmosphere-ocean coupling associated

with ENSO, which can also be used as a predictor for ENSO impacts on the extratropics (Chiodi & Harrison, 2013, 2015; L'Heureux et al., 2015). Clarke (2014) argued that anomalous deep convective heating is essential for the coupled development of El Niño by generating anomalous surface equatorial westerly winds that push the warm water further eastward, leading to more anomalous deep convection and stronger westerly wind anomalies, and thereby, promoting the growth of ocean-atmosphere instability.

Interestingly, oceanic warming extended from 150°E eastward to the South American coast during the four uncoupled events. The major warming center was located around 120°W during 1979/1980 and 180° in 2004. During 2014/2015 and 2018, in contrast, there were two warming centers, which were located in the CP and EP, respectively. Such SSTA distributions exhibit smaller SSTA zonal gradients across the tropical Pacific than typically associated with El Niño. These characteristics of the four uncoupled warming events are consistent with the corresponding composites of SST and low-level wind (Figure 3b) for Niño3.4 $\geq$ 0.5 °C and CP_OLR index $\geq$0.0 W/m^2 (see the green bars in Figure 2). The maximum SSTAs are in the central (170°E to 180°) and eastern central (150–120°W) tropical Pacific, respectively, and weak low-level convergence in the central and eastern tropical Pacific. Such a pattern is somewhat similar to CP El Niño (or warm pool El Niño/Modoki; Ashok et al., 2007; Z.-Z. Hu et al., 2012; Kao & Yu, 2009; Kug et al., 2009; Yeh et al., 2009). However, CP El Niño events have active atmosphere-ocean coupling (including Bjerknes feedbacks and recharge/discharge oscillations; Kug et al., 2009; Ren & Jin, 2013). In contrast, the corresponding composites (Figure 3a) for Niño3.4 $\geq$ 0.5 °C and CP_OLR index <0.0 W/m^2 (see the yellow bars in Figure 2) look like an EP El Niño pattern.

In fact, in addition to linking with Niño3.4 SSTA (Figure 3c), the deep convection anomaly in the central tropical Pacific is also tied to the zonal gradient of SSTA across the tropical Pacific (Figure 3d). Based on the SSTA distribution in the four uncoupled warming events and the composites (Figures 1 and 3b), we define a zonal SST gradient index as the SSTA difference between the central (5°S to 5°N, 160°E to 160°W) and eastern (5°S to 5°N, 120–90°W) tropical Pacific (green rectangles in Figure 3b). In previous studies, the zonal gradient of SSTA across the tropical Pacific, such as the Niño4 and Niño3 index difference, was used to identify and characterize different flavors of El Niño (Kug et al., 2009; Yeh et al., 2009). Statistically, the correlation between the CP_OLR index and the SSTA zonal gradient index reaches its maximum positive value at zero-month lead (bars in Figure 3d), meaning that when the anomalous warming is stronger in the central tropical Pacific than in the eastern tropical Pacific, deep convection in the central tropical Pacific is suppressed. The results are similar if the CP_OLR index was defined in a slightly different region, such as the Niño4 or Niño3.4 regions (not shown), implying robustness of the results.

According to Lindzen and Nigam (1987), the zonal gradient of SSTA in the tropical Pacific can generate low-level wind and convergence/divergence anomalies via the zonal gradient of air surface pressure. In agreement with this hypothesis, in addition to the statistical connection with the convection over the central tropical Pacific and the SSTA zonal gradient index (Figure 3d), the SSTA zonal gradient index is also linked to the zonal wind anomalies (Figure 3e). Statistically, larger anomalous warming in the central tropical Pacific than in the eastern tropical Pacific favors easterly wind anomalies in the eastern tropical Pacific. For the four uncoupled warming events, the zonal distribution of SSTA across the tropical Pacific associated with an overall positive or small zonal gradient of SSTA was unfavorable for the development of deep convection and surface westerly wind anomalies in the central tropical Pacific, which led to the failure of atmosphere-ocean coupling. Thus, in addition to the warming intensity, the spatial pattern of the warming in the tropical Pacific is also crucial in triggering and enhancing the deep convection in the central tropical Pacific to initiate atmosphere-ocean coupling. Thus, anomalous warming of the eastern tropical Pacific alone is not sufficient to guarantee the onset of the ocean-atmosphere coupling characteristic of ENSO.

The uncoupled warming events, in which the warming in Niño3.4 is not accompanied by the corresponding atmosphere anomalies, are unusual in the spectrum of ENSO diversity. The hypothesis about the decoupling and tropical Pacific zonal gradient of SST is consistent with previous work. For example, McPhaden (2012) and Hu et al. (2013) identified a regime shift in ENSO variability with a decrease of the amplitude and an increase of the frequency of ENSO since 1999/2000. Z.-Z. Hu et al. (2013) and Z.-Z. Hu, Kumar, Huang, et al. (2020) argued that this regime shift was associated with a strengthening in the zonal mean climate state contrast between the western and eastern tropical Pacific and a westward shift in the crucial atmosphere-ocean coupling region (Z.-Z. Hu, Kumar, Huang, et al., 2020; Li, Hu, & Becker, 2019;

Lübbecke & McPhaden, 2014). Johnson et al. (2019) proposed that delayed occurrences of the atmospheric and oceanic coupling in weak El Niño events (2014/2015 and 2018/2019) was linked to the tendency of SST zonal gradient between the western and central equatorial Pacific that has strengthened significantly since 1979. The strengthened zonal gradient produces an atmospheric response that opposes the response to elevated EP SSTs and inhibits the expected onset of central tropical Pacific deep convection during 2014/2015 and 2018/2019 events. Through climate model experiments, Lim et al. (2019) also suggested that strength of extreme El Niño events (1982/1983, 1997/1998, and 2015/2016) was reduced with a strengthened zonal contrast as the result of reduced thermocline feedback and weakened rainfall-wind-SST coupling over the tropical EP, which is also consistent with the simple model results of Z.-Z. Hu et al. (2013; see their Figure 6). However, the relative importance of the zonal SSTA gradient and the amplitude of the SSTA is yet to be robustly and quantitatively estimated, due to the fact that just four cases of uncoupled El Niño have been observed.

In this regard, we note that another common factor of the four uncoupled warming events is their late start. All four events started in August–October as measured by SST exceeding 0.5 °C for the first time (Figure 1). This late onset corresponds to a climatologically well-established cold tongue and the largest season mean zonal SST gradient on the equator. These conditions could also limit the eastward extension of deep convection, confining enhanced precipitation to the far western Pacific south of the equator (Figure 4b) thus limiting the coupling of the atmosphere and ocean coupling in the tropical CP and EP.

4. Different Impact on Extratropical Climate

Without the corresponding eastward shift of deep convection during uncoupled warming events, the impact of the ocean warming in the central and eastern tropical Pacific is unable to affect the extratropics (Chiodi & Harrison, 2013, 2015; Yeh et al., 2018). For the El Niño composite (Figure 4a), the rainfall is above normal in the central and eastern tropical Pacific and below normal in the western tropical Pacific. This pattern is an indication of the eastward shift in the strongest tropical Pacific deep convection and heavy rainfall, consistent with the corresponding composites of SST and low-level wind anomalies (Figure 3a). In the extratropics, the El Niño composite precipitation pattern is consistent with previous work, such as Davey et al. (2014; see their Figure 13). Precipitation anomalies in the uncoupled warming event composite (Figure 4b), in contrast, show smaller spatial scales and less organized spatial structure. For the composite of the uncoupled warming events, below-normal rainfall in the tropics is primarily confined to the northwestern Pacific, while the anomaly is relatively small along the equator compared with the El Niño composite. In the extratropics, there are few areas of significant rainfall anomalies, which may not be robust due to the small sample size in the uncoupled warming event composite and the absence of the tropical forcing in the CP. It should be pointed out that these uncoupled warming events are weak as well, suggesting that the intensity of El Niño may also matter for the differences shown in Figures 3a, 3b, 4a, and 4b.

We use North America as an example to illustrate the differences in the extratropics in the composites of El Niño and uncoupled warming events. The precipitation anomaly pattern in the El Niño composite features opposing anomalies between the northern and southern portions of the continent: above normal in the south and below normal in the north (45–60°N) (Figure 4a), which is similar to the impact of EP El Niño (e.g., Yu & Zou, 2013). In contrast, the uncoupled warming event composite anomaly (Figure 4b) is less coherent and noisier. Such contrasting anomaly patterns imply that we cannot well predict the precipitation anomaly pattern in North America based on elevated SSTs in the tropical Pacific alone, since the presence or absence of atmosphere-ocean coupling appears to be a crucial factor as well.

5. Challenges for Prediction

Currently, most of the operational climate prediction centers, such as CPC (http://origin.cpc.ncep.noaa.gov/products/analysis_monitoring/ensostuff/ONI_v5.php), International Research Institute for Climate and Society of Columbia University (https://iri.columbia.edu/our-expertise/climate/forecasts/enso/current/?enso_tab=enso-sst_table), and Australian Bureau of Meteorology (http://www.bom.gov.au/climate/ocean/outlooks/#region=NINO34), rely on some oceanic indices (e.g., Niño3.4 SSTA index) as the underpinning for ENSO forecasts and monitoring. In reality, these simple SSTA indices sometimes fail to reflect the coupling between the atmosphere and ocean. Furthermore, ocean warming in the central and eastern

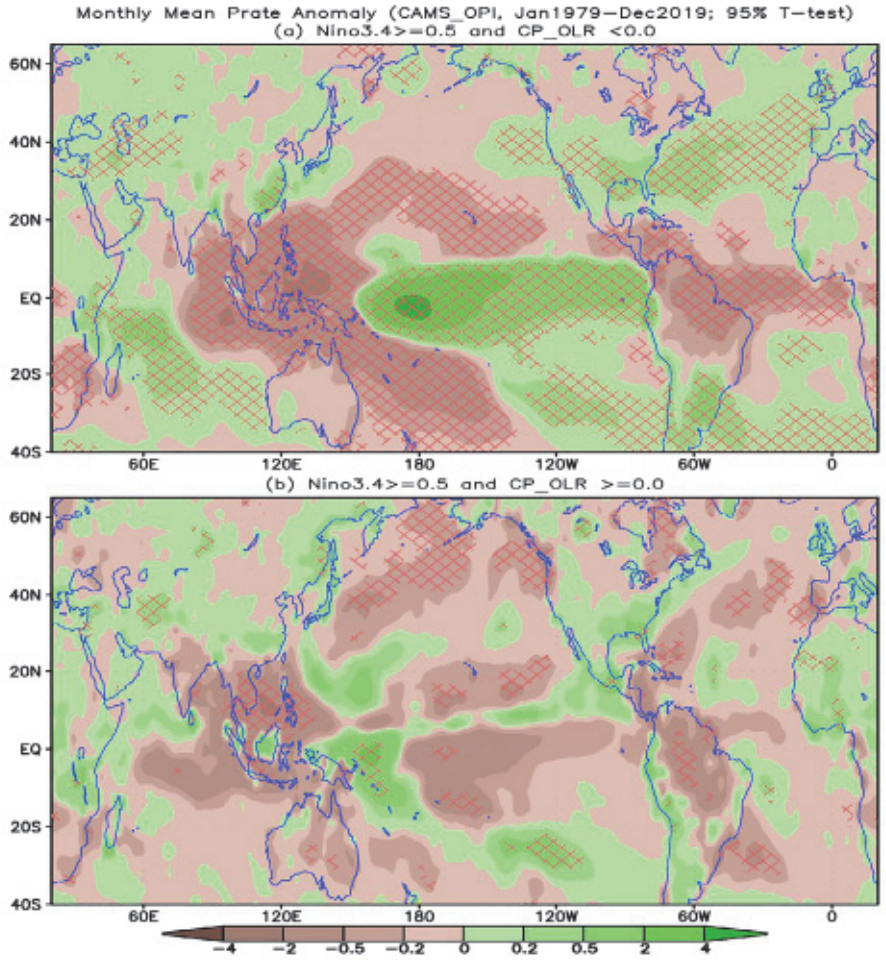

Figure 4. Composites of monthly mean precipitation anomalies for (a) Niño3.4 ≥ 0.5 °C and CP_OLR < 0.0, and (b) Niño3.4 ≥ 0.5 °C and CP_OLR > 0.0 during January 1979 to December 2019. Monthly data were used in the composites, which include 111 months in (a) and 28 months in (b), respectively. The hatches indicate that the composite anomalies are significantly different at 5% level from those of the nonselected month based on a *t* test. The unit is mm/day.

tropical Pacific has different impacts on the extratropics for cases with and without atmosphere-ocean coupling, which makes it necessary to distinguish coupled from uncoupled warming events to determine the likely skill in forecasting far-field teleconnections.

To capture the coupled or uncoupled warming, our results suggest that correct prediction of the zonal SSTA gradient is crucial. In operational model forecasts, the prediction skill of the zonal SSTA gradient across the equatorial Pacific (the zonal SSTA gradient index) is much lower than that of the Niño3.4 index. For example, in 0- to 8-month lead forecasts of Climate Forecast System Version 2, the skill, measured by the linear correlation between the ensemble forecast and observations for all initial and target months, is in a range of 0.64–0.89 for the Niño3.4 index and ~0.18–0.83 for the zonal SSTA gradient index, with a faster decline in skill for the zonal gradient index with increasing lead time (Figure S3). The lower skill in predicting the zonal SSTA gradient, and thus active convection in the central equatorial Pacific and the associated atmosphere-ocean coupling, is a challenge for climate models.

Furthermore, forecasting climate variability seems more difficult during uncoupled warming events than during bone fide El Niños. Here, we use official CPC forecasts for monthly mean precipitation and temperature over the United States during January 1995 to December 2019 as an example. The averaged HSS is highest in El Niño months (Niño3.4 ≥ 0.5 °C and CP-OLR < 0) and lowest in uncoupled El Niño warming

months, with intermediate skill in ENSO neutral months for precipitation (Figure S4). In the official forecasts, ENSO and lower-frequency variations (or trends) are the two most important predictors (O'Lenic et al., 2008; Peng et al., 2013). The ENSO impact in the official forecasts predominantly relies on the composites, which are solely based on the Niño3.4 index without considering whether the atmosphere and the ocean are coupled in the tropical Pacific.

We note that the sign of precipitation anomalies is opposite in most regions of the northern contiguous United States between the composites with and without CP convection (Figure 4) though in both cases Niño3.4 $\geq$ 0.5 °C. Thus, using the composite anomalies shown in Figure 4a to make forecasts for the cases when CP convection is absent would result in degraded skill of the forecasts. Basically, that is the situation of the current forecast operation at CPC, which highlights the necessity to distinguish coupled and uncoupled El Niños. This conclusion is consistent with some previous studies, such as Chiodi and Harrison (2013, 2015). For their OLR-ENSO events composite, winter precipitation anomalies over the global land are robust (i.e., statistically significant over large areas), while there are very few statistically significant seasonal precipitation anomalies associated with the non-OLR-ENSO events. Further comparing the CPC official forecast skill for El Niño and neutral events, we note that the relative difference is larger for precipitation forecasts (line in Figure S4), while the temperature forecast skills are comparable between El Niño and neutral events (bars in Figure S4). These results imply that for precipitation forecasts, El Niño is more important than other factors in determining skill, while for temperature, other factors, such as the long-term trend, make more substantial contributions to temperature forecast skill than El Niño.

Lastly, it is still a challenge to accurately describe atmospheric and oceanic coupling processes associated with ENSO in reanalyses and in climate forecast systems. For example, Kumar and Hu (2012) found large differences among reanalyses for the intensity and the spatial structure of ocean-atmosphere feedback terms involving precipitation, surface wind stress, and ocean surface heat flux associated with ENSO. For climate forecast models, tropical convection and ENSO evolution are sensitive to the parameterization of atmospheric convection. Zhu et al. (2017) noted a substantial sensitivity of the SST prediction skill to different convection schemes, particularly over the eastern tropical Pacific. They argued that the convection scheme having the highest skill simulates stronger and more realistic coupled feedbacks related to ENSO. Thus, accurately representing the different mechanisms responsible for different flavors of ENSO and their global impacts in climate models represents a significant challenge for climate prediction.

Acknowledgments
We thank two anonymous reviewers and Drs. Yun Fan and Hui Wang for their constructive suggestions and insightful comments. This is PMEL Contribution 4995. J. Y. Y. was supported by NSF's Climate and Large-Scale Dynamics Program under Grant AGS-1833075. N. C. J. was supported under Award NA14OAR4320106 from the NOAA, U. S. Department of Commerce. All data used in this work are available online: SST, D20, R2 surface wind, and OLR (from https://www.esrl.noaa.gov/psd/data/gridded); precipitation data (from https://iridl.ldeo.columbia.edu/SOURCES/.NOAA/.NCEP/.CPC/.CAMS_OPI/.v0208/index.html?Set-Language=en); CFSv2 forecasts from (https://rda.ucar.edu/datasets/ds094.2); CPC operational forecast skill of monthly temperature and precipitation (from https://www.cpc.ncep.noaa.gov/products/predictions/long_range/tools/briefing/mon_veri.grid.php); and CFSv2 forecasts (from https://rda.ucar.edu/datasets/ds094.2).

References

Ashok, K., Behera, S. K., Rao, S. A., Weng, H., & Yamagata, T. (2007). El Niño Modoki and its possible teleconnection. *Journal of Geophysical Research*, *112*, C11007. https://doi.org/10.1029/2006JC003798

Barnston, A. G., Tippett, M. K., L'Heureux, M. L., Li, S., & DeWitt, D. G. (2012). Skill of real-time seasonal ENSO model predictions during 2002–2011—Is our capability increasing? *Bulletin of the American Meteorological Society*, *93*(5), 631–651. https://doi.org/10.1175/BAMS-D-11-00111.1

Battisti, D. S., & Hirst, A. C. (1989). Interannual variability in a tropical atmosphere-ocean model. Influence of the basic state, ocean geometry and nonlinearity. *Journal of the Atmospheric Sciences*, *46*, 1687–1712. https://doi.org/10.1175/1520-0469(1989)046<1687:IVIATA>2.0.CO;2

Bjerknes, J. (1969). Atmospheric teleconnections from the equatorial Pacific. *Monthly Weather Review*, *97*, 163–172. https://doi.org/10.1175/1520-0493(1969)097<0163:ATFTEP>2.3.CO;2

Bretherton, C. S., Widmann, M., Dymnikov, V. P., Wallace, J. M., & Blade, I. (1999). Effective number of degrees of freedom of a spatial field. *Journal of Climate*, *12*, 1990–2009. https://doi.org/10.1175/1520-0442(1999)012<1990:TENOSD>2.0.CO;2

Cane, M. A., Munnich, M., & Zebiak, S. E. (1990). A study of self-excited oscillations of the tropical ocean–atmosphere system. Part I: Linear analysis. *Journal of the Atmospheric Sciences*, *47*, 1562–1577. https://doi.org/10.1175/1520-0469(1991)048<1238:ASOSEO>2.0.CO;2

Capotondi, A., Wittenberg, A. T., Newman, M., di Lorenzo, E., Yu, J. Y., Braconnot, P., et al. (2015). Understanding ENSO diversity. *Bulletin of the American Meteorological Society*, *96*(6), 921–938. https://doi.org/10.1175/BAMS-D-13-00117.1

Chen, D., Lian, T., Fu, C., Cane, M. A., Tang, Y., Murtugudde, R., et al. (2015). Strong influence of westerly wind bursts on El Niño diversity. *Nature Geoscience*, *8*, 339–345. https://doi.org/10.1038/ngeo2399

Chiodi, A. M., & Harrison, D. E. (2013). El Niño impacts on seasonal U. S. atmospheric circulation, temperature, and precipitation anomalies: The OLR-event perspective. *Journal of Climate*, *26*, 822–837. https://doi.org/10.1175/JCLI-D-12-00097.1

Chiodi, A. M., & Harrison, D. E. (2015). Global seasonal precipitation anomalies robustly associated with El Niño and La Niña events—An OLR perspective. *Journal of Climate*, *28*, 6133–6159. https://doi.org/10.1175/JCLI-D-14-00387.1

Clarke, A. J. (2014). El Niño physics and El Niño predictability. *Annual Review of Marine Science*, *6*, 79–99. https://doi.org/10.1146/annurev-marine-010213-135026

Clement, A., Di Nezio, P., & Deser, C. (2011). Rethinking the ocean's role in the Southern Oscillation. *Journal of Climate*, *24*, 4056–4072. https://doi.org/10.1175/2011JCLI3973.1

Davey, M. K., Brookshaw, A., & Ineson, S. (2014). The probability of the impact of ENSO on precipitation and near-surface temperature. *Climate Risk Management*, *1*, 5–24. https://doi.org/10.1016/j.crm.2013.12.002

Dommenget, D. (2010). The slab ocean El Niño. *Geophysical Research Letters*, *37*, L20701. https://doi.org/10.1029/2010GL044888

Hu, S., & Fedorov, A. V. (2016). Exceptional strong easterly wind burst stalling El Niño of 2014. *Proceedings of the National Academy of Sciences*, *113*(8), 2005–2010. https://doi.org/10.1073/pnas.1514182113

Hu, Z.-Z., Huang, B., Zhu, J., Kumar, A., & McPhaden, M. J. (2019). On the variety of coastal El Niño events. *Climate Dynamics*, *52*(12), 7537–7552. https://doi.org/10.1007/s00382-018-4290-4

Hu, Z.-Z., Kumar, A., Huang, B., Zhu, J., L'Heureux, M., McPhaden, M. J., & Yu, J.-Y. (2020). The interdecadal shift of ENSO properties in 1999/2000: A review. *Journal of Climate*. https://doi.org/10.1175/JCLI-D-19-0316.1

Hu, Z.-Z., Kumar, A., Jha, B., & Huang, B. (2020). How much of monthly mean precipitation variability over global land is associated with SST anomalies? *Climate Dynamics*, *54*(1–2), 701–712. https://doi.org/10.1007/s00382-019-05023-5

Hu, Z.-Z., Kumar, A., Jha, B., Wang, W., Huang, B., & Huang, B. (2012). An analysis of warm pool and cold tongue El Niños: Air-sea coupling processes, global influences, and recent trends. *Climate Dynamics*, *38*(9–10), 2017–2035. https://doi.org/10.1007/s00382-011-1224-9

Hu, Z.-Z., Kumar, A., Ren, H.-L., Wang, H., L'Heureux, M., & Jin, F.-F. (2013). Weakened interannual variability in the tropical Pacific Ocean since 2000. *Journal of Climate*, *26*(8), 2601–2613. https://doi.org/10.1175/JCLI-D-12-00265.1

Hu, Z.-Z., Kumar, A., Zhu, J., Peng, P., & Huang, B. (2019). On the challenge for ENSO cycle prediction: An example from NCEP Climate Forecast System version 2. *Journal of Climate*, *32*(1), 183–194. https://doi.org/10.1175/JCLI-D-18-0285.1

Huang, B., Xue, Y., Zhang, D., Kumar, A., & McPhaden, M. J. (2010). The NCEP GODAS ocean analysis of the tropical Pacific mixed layer heat budget on seasonal to interannual time scales. *Journal of Climate*, *23*, 4901–4925.

Janowiak, J. E., & Xie, P. (1999). CAMS_OPI: A global satellite-rain gauge merged product for real-time precipitation monitoring applications. *Journal of Climate*, *12*, 3335–3342.

Jin, F.-F. (1997a). An equatorial ocean recharge paradigm for ENSO. Part I: Conceptual model. *Journal of the Atmospheric Sciences*, *54*, 811–829. https://doi.org/10.1175/1520-0469(1997)054<0811:AEORPF>2.0.CO;2

Jin, F.-F. (1997b). An equatorial ocean recharge paradigm for ENSO. Part II: A stripped-down coupled model. *Journal of the Atmospheric Sciences*, *54*, 830–847. https://doi.org/10.1175/1520-0469(1997)054<0830:AEORPF>2.0.CO;2

Johnson, N. C., L'Heureux, M. L., Chang, C.-H., & Hu, Z.-Z. (2019). On the delayed coupling between ocean and atmosphere in recent weak El Niño episodes. *Geophysical Research Letters*, *46*, 11,416–11,425. https://doi.org/10.1029/2019GL084021

Johnson, N. C., & Xie, S.-P. (2010). Changes in the sea surface temperature threshold for tropical convection. *Nature Geoscience*, *3*, 842–845. https://doi.org/10.1038/ngeo1008

Kanamitsu, M., Ebisuzaki, W., Woollen, J., Yang, S.-K., Hnilo, J. J., Fiorino, M., & Potter, G. L. (2002). NCEP/DOE AMIP-II Reanalysis (R-2). *Bulletin of the American Meteorological Society*, *83*, 1631–1643. https://doi.org/10.1175/BAMS-83-11-1631

Kao, H.-Y., & Yu, J.-Y. (2009). Contrasting eastern-Pacific and central-Pacific types of ENSO. *Journal of Climate*, *22*, 615–632. https://doi.org/10.1175/2008JCLI2309.1

Kug, J.-S., Jin, F.-F., & An, S.-I. (2009). Two types of El Niño events: Cold tongue El Niño and warm pool El Niño. *Journal of Climate*, *22*, 1499–1515. https://doi.org/10.1175/2008JCLI2624.1

Kumar, A., & Hu, Z.-Z. (2012). Uncertainty in the ocean-atmosphere feedbacks associated with ENSO in the reanalysis products. *Climate Dynamics*, *39*(3–4), 575–588. https://doi.org/10.1007/s00382-011-1104-3

L'Heureux, M. L., Tippett, M. K., & Barnston, A. G. (2015). Characterizing ENSO coupled variability and its impact on North American seasonal precipitation and temperature. *Journal of Climate*, *28*, 4231–4245. https://doi.org/10.1175/JCLI-D-14-00508.1

Li, X., Hu, Z.-Z., & Becker, E. (2019). On the westward shift of tropical Pacific climate variability since 2000. *Climate Dynamics*, *53*(5–6), 2905–2918. https://doi.org/10.1007/s00382-019-04666-8

Li, X., Hu, Z.-Z., & Huang, B. (2019). Contributions of atmosphere-ocean interaction and low-frequency variation to intensity of strong El Niño events since 1979. *Journal of Climate*, *32*(5), 1381–1394. https://doi.org/10.1175/JCLI-D-18-0209.1

Liebmann, B., & Smith, C. A. (1996). Description of a complete (interpolated) outgoing longwave radiation dataset. *Bulletin of the American Meteorological Society*, *77*, 1275–1277. https://doi.org/10.1175/1520-0477-77.6.1274

Lim, E.-P., Hendon, H., Hope, P., Chung, C., Delage, F., & McPhaden, M. (2019). Continuation of tropical Pacific Ocean temperature trend may weaken extreme El Niño and its linkage to the Southern Annular Mode. *Scientific Reports*, *9*(1), 1–15. https://doi.org/10.1038/s41598-019-53371-3

Lindzen, R. S., & Nigam, S. (1987). On the role of sea surface temperature gradients in forcing low-level winds and convergence in the tropics. *Journal of the Atmospheric Sciences*, *44*, 2440–2458. https://doi.org/10.1175/1520-0469(1987)044<2418:OTROSS>2.0.CO;2

Lübbecke, J. F., & McPhaden, M. J. (2014). Assessing the 21st century shift in ENSO variability in terms of the Bjerknes stability index. *Journal of Climate*, *27*, 2577–2587. https://doi.org/10.1175/JCLI-D-13-00438.1

McPhaden, M. J. (1999). Genesis and evolution of the 1997–98 El Niño. *Science*, *283*(5404), 950–954. https://doi.org/10.1126/science.283.5404.950

McPhaden, M. J. (2012). A 21st century shift in the relationship between ENSO SST and warm water volume anomalies. *Geophysical Research Letters*, *39*, L09706. https://doi.org/10.1029/2012GL051826

McPhaden, M. J. (2015). Playing hide and seek with El Niño. *Nature Climate Change*, *5*(9), 791–795. https://doi.org/10.1038/nclimate2775

Meinen, C. S., & McPhaden, M. J. (2000). Observations of warm water volume changes in the equatorial Pacific and their relationship to El Niño and La Niña. *Journal of Climate*, *13*, 3551–3559. https://doi.org/10.1175/1520-0442

National Research Council. (2010): Assessment of intraseasonal to interannual climate prediction and predictability. Washington, D. C., USA: National Academies Press

O'Lenic, E. A., Unger, D. A., Halpert, M. S., & Pelman, K. S. (2008). Developments in operational long-range climate prediction at CPC. *Weather Forecasting*, *23*, 496–515. https://doi.org/10.1175/2007WAF2007042.1

Peng, P., Barnston, A. G., & Kumar, A. (2013). A comparison of skill between two versions of the NCEP Climate Forecast System (CFS) and CPC's operational short-Lead seasonal outlooks. *Weather Forecasting*, *28*, 445–462. https://doi.org/10.1175/WAF-D-12-00057.1

Picaut, J., Ioualalen, M., Menkes, C., Delcroix, T., & McPhaden, M. J. (1996). Mechanism of the zonal displacements of the Pacific warm pool: Implications for ENSO. *Science*, *274*, 1486–1489.

Ren, H.-L., & Jin, F.-F. (2013). Recharge oscillator mechanisms in two types of ENSO. *Journal of Climate*, *26*, 6506–6523. https://doi.org/10.1175/JCLI-D-12-00601.1

Reynolds, R. W., Rayner, N. A., Smith, T. M., Stokes, D. C., & Wang, W. (2002). An improved in situ and satellite SST analysis for climate. *Journal of Climate*, *15*, 1609–1625. https://doi.org/10.1175/1520-0442(2002)015<1609:AIISAS>2.0.CO;2

Saha, S., Moorthi, S., Wu, X., Wang, J., Nadiga, S., Tripp, P., et al. (2014). The NCEP Climate Forecast System Version 2. *Journal of Climate*, *27*(6), 2185–2208. https://doi.org/10.1175/JCLI-D-12-00823.1

Santoso, A., McPhaden, M. J., & Cai, W. (2017). The defining characteristics of ENSO extremes and the strong 2015/2016 El Niño. *Reviews of Geophysics*, *55*, 1079–1129. https://doi.org/10.1002/2017RG000560

Sarachik, E. S., & Cane, M. A. (2010). *The El Niño-Southern Oscillation Phenomenon*, (p. 384). London: Cambridge University Press.

Suarez, M. J., & Schopf, P. S. (1988). A delayed action oscillator for ENSO. *Journal of the Atmospheric Sciences*, *45*, 3283–3287. https://doi.org/10.1175/1520-0469(1988)045<3283:ADAOFE>2.0.CO;2

Timmermann, A., An, S.-I., Kug, J.-S., Jin, F.-F., Cai, W., Capotondi, A., et al. (2018). El Niño–southern oscillation complexity. *Nature*, *559* (7715), 535–545. https://doi.org/10.1038/s41586-018-0252-6

Wang, C. (2001). A unified oscillator model for the El Niño–Southern Oscillation. *Journal of Climate*, *14*, 98–115. https://doi.org/10.1175/1520-0442(2001)014<0098:AUOMFT>2.0.CO;2

Wang, C. (2018). A review of ENSO theories. *National Science Review*, *5*(6), 813–825. https://doi.org/10.1093/nsr/nwy104

Wang, C., Deser, C., Yu, J.-Y., DiNezio, P., & Clement, A. (2016). El Niño–Southern Oscillation (ENSO): A review. In P. Glynn, D. Manzello, & I. Ecnochs (Eds.), *Coral reefs of the eastern Pacific*, (pp. 85–106). Berlin/Heidelber: Springer Science Publisher.

Wyrtki, K. (1985). Water displacements in the Pacific and the genesis of El Niño cycles. *Journal of Geophysical Research*, *90*(C4), 7129–7132. https://doi.org/10.1029/JC090iC04p07129

Yeh, S., Kug, J., Dewitte, B., Kwon, M., Kirtman, B. P., & Jin, F.-F. (2009). El Niño in a changing climate. *Nature*, *461*(7263), 511–514. https://doi.org/10.1038/nature08316

Yeh, S.-W., Cai, W., Min, S.-K., McPhaden, M. J., Dommenget, D., Dewitte, B., et al. (2018). ENSO atmospheric teleconnections and their response to greenhouse gas forcing. *Reviews of Geophysics*, *56*, 185–206. https://doi.org/10.1002/2017RG000568

Yu, J.-Y., & Zou, Y. (2013). The enhanced drying effect of Central-Pacific El Niño on US winter. *Environmental Research Letters*, *8*. https://doi.org/10.1088/1748-9326/8/1/014019

Zheng, Z., Hu, Z.-Z., & L'Heureux, M. (2016). Predictable components of ENSO evolution in real-time multi-model predictions. *Scientific Reports*, *6*(1), 1–9. https://doi.org/10.1038/srep35909

Zhu, J., Kumar, A., Wang, W., Hu, Z.-Z., Huang, B., & Balmaseda, M. A. (2017). Importance of convection parameterization in ENSO predictions. *Geophysical Research Letters*, *44*, 6334–6342. https://doi.org/10.1002/2017GL073669